

Layer with reduced viscosity at water-oil interfaces probed by fluorescence correlation spectroscopyDapeng Wang,¹ Leonid Pevzner,¹ Chen Li,¹ Kalina Peneva,¹ Christopher Y. Li,² Derek Y. C. Chan,^{3,4} Klaus Müllen,¹ Markus Mezger,¹ Kaloian Koynov,^{1,*} and Hans-Jürgen Butt¹¹Max-Planck Institute for Polymer Research, Ackermannweg 10, 55128 Mainz, Germany²Department of Materials Science and Engineering, Drexel University, Philadelphia 19104, USA³Department of Mathematics and Statistics and Particulate Fluids Processing Centre, University of Melbourne, Parkville, 3010, Australia⁴Faculty of Life and Social Sciences, Swinburne University of Technology, Hawthorn 3122, Australia

(Received 24 February 2012; revised manuscript received 26 September 2012; published 3 January 2013)

The two-dimensional diffusion of isolated molecular tracers at the water-*n*-alkane interface was studied with fluorescence correlation spectroscopy. The interfacial diffusion coefficients of larger tracers with a hydrodynamic radius of 4.0 nm agreed well with the values calculated from the macroscopic viscosities of the two bulk phases. However, for small molecule tracers with hydrodynamic radii of only 1.0 and 0.6 nm, notable deviations were observed, indicating the existence of an interfacial region with reduced effective viscosity and increased mobility.

DOI: [10.1103/PhysRevE.87.012403](https://doi.org/10.1103/PhysRevE.87.012403)

PACS number(s): 68.05.Cf, 68.43.Jk, 87.80.Nj

I. INTRODUCTION

Water is the most common liquid on Earth and constitutes a major part of living organisms. Not surprisingly, therefore, its structure, properties, and interactions with other substances have been continuously studied from ancient times to nowadays. One particularly interesting question is what exactly happens when water meets hydrophobic molecules or surfaces [1,2]. The term hydrophobic is commonly used to describe nonpolar molecules, e.g., *n*-alkanes (or oils in general) that, when mixed with water, separate into water-rich and oil-rich phases. The reason for separation is the fact that nonpolar molecules are not able to form hydrogen bonds with the polar water molecules. As a result, water repels them in favor of bonding with itself to form a randomly fluctuating network [1,3]. Proximity of water to an extended hydrophobic surface, however, disrupts the hydrogen-bonding pattern, as supported by existence of dangling OH bonds, and thus changes the water properties near the interface [4–7]. Theoretical considerations suggested the presence of a region of reduced water density adjacent to hydrophobic moieties [1,8,9]. Indeed, on solid hydrophobic surfaces this so-called “hydrophobic gap” has been observed experimentally by x ray [10–13], by neutron reflectivity [14], and confirmed by computer simulations [15]. The overall picture emerging from these studies is consistent with an interfacial depletion length corresponding to less than a monolayer of water. The origin of the observed molecular scale depletion includes contributions from the reduced density of terminal methyl groups [16], generic packing effects of liquids adjacent to a solid wall [17], and the complex interplay between the water structure and the topography of the hydrophobic surface [13,15].

With respect to fluid water-hydrophobic interfaces, in 1994 Du and coworkers found that the sum frequency generation spectra in the OH-bonding region at the water-*n*-hexane interface exhibit a large similarity with the signal from the liquid-vapor surface while those recorded on a hydrophobic solid substrate show remarkable differences [4]. Today this difference is commonly attributed to a different arrangement

of water molecules near a thermally fluctuating fluid interface compared to a rigid hard wall [18]. These differences may also be the reason why theoretical [19–21] and experimental [22,23] studies reported controversial results on the existence of a depletion layer at liquid-liquid interfaces. To rationalize the situation, new data, preferably obtained with complementary experimental techniques, are required.

Here, we applied the technique of fluorescence correlation spectroscopy (FCS) [24] to study the diffusion of tracer molecules with different sizes at water-*n*-alkane interfaces and explored the properties of the interfacial layer. Compared to other techniques, FCS is well suited as it offers the possibility to monitor subnanometer size objects with high mobility at very low surface coverage [25].

II. EXPERIMENTAL DETAILS

All *n*-alkanes were purchased from Sigma-Aldrich and purified following a procedure described in the literature [26]. For the aqueous phase either pure Milli-Q water or Milli-Q water-glycerol mixtures with 5, 10, 20, and 30 vol % glycerol were used. Glycerol was purchased from Sigma-Aldrich and used without further purification. To degas the liquids, vacuum was applied to liquid flasks with a Teflon stirrer. Continuous stirring was used to shake off the bubbles nucleated on the surface of the Teflon stirrer. The system was kept under vacuum for longer than 2 h until no bubble formation was seen on the Teflon stirrer [27].

As tracers we used water soluble, fluorescent core-shell dendrimer molecules with a hydrodynamic radius of $R_H = 4.0$ nm and the smaller PDI1 ($R_H = 1.0$ nm) and Rhodamine 6G ($R_H = 0.6$ nm) dye molecules. Their chemical structures are presented in Fig. 1. The Rhodamine 6G was purchased from Sigma-Aldrich. The water-soluble perylene dye PDI1 and the PDI-G1-PAEMA dendrimer were prepared as described previously [28,29]. The rhodamine is a standard dye, commonly used in fluorescence correlation spectroscopy (FCS) studies and its hydrodynamic radius is known from previous studies [30]. The hydrodynamic radii of the PDI1 and the dendrimer were measured by FCS in bulk water.

The water-*n*-alkane interfaces were prepared in an Attofluor cell chamber (Invitrogen, Leiden, Netherlands) with

*Corresponding author: koynov@mpip-mainz.mpg.de

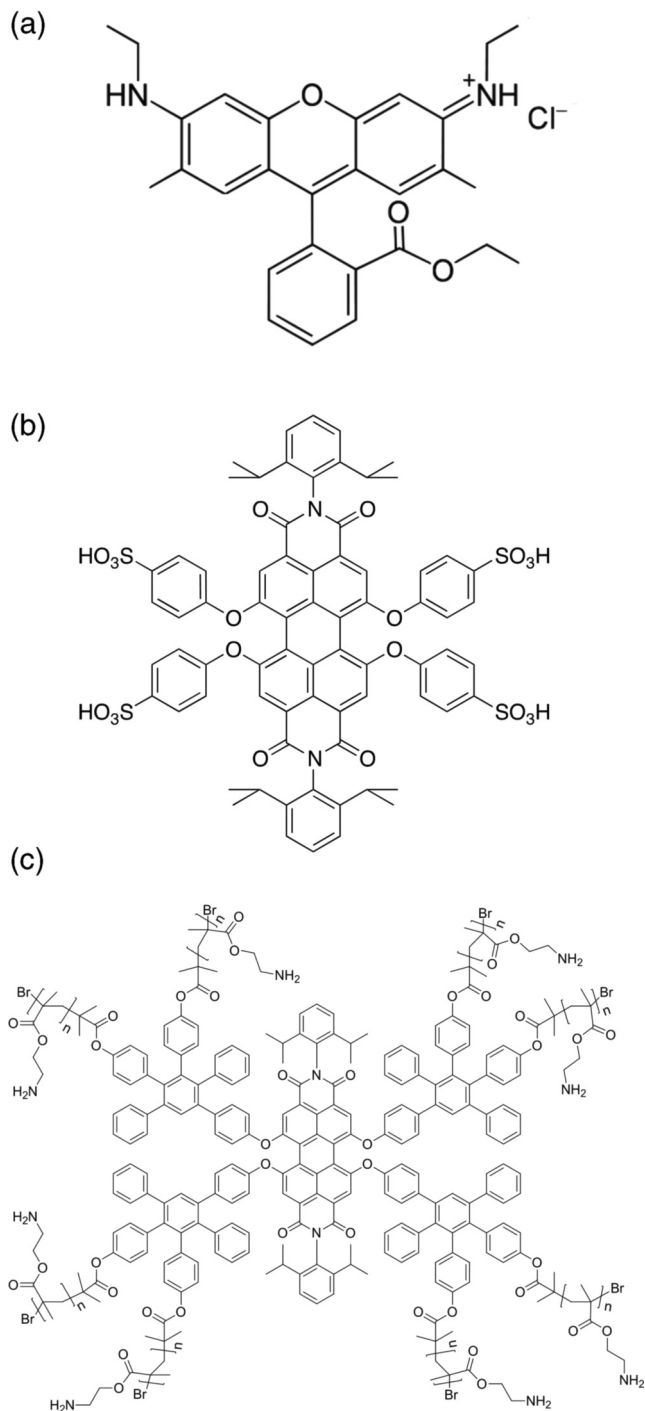


FIG. 1. Chemical structures of the used tracers: (a) rhodamine, (b) PDI1, and (c) dendrimer.

a thin microscope cover glass bottom. An aluminum foil O-ring with inner diameter of 0.5 cm and thickness of approximately 0.3 mm was fixed on the cover glass to restrict the sample volume and surface. This O-ring was first filled with degassed water to a height of approximately 100 μm . Then a drop of 0.5- μl aqueous solution of the fluorescent tracer molecules with a concentration of 10^{-11} M was added. Finally, the alkane phase was carefully added on top of the aqueous phase. The tracer molecules absorbed fast on the interface, reaching

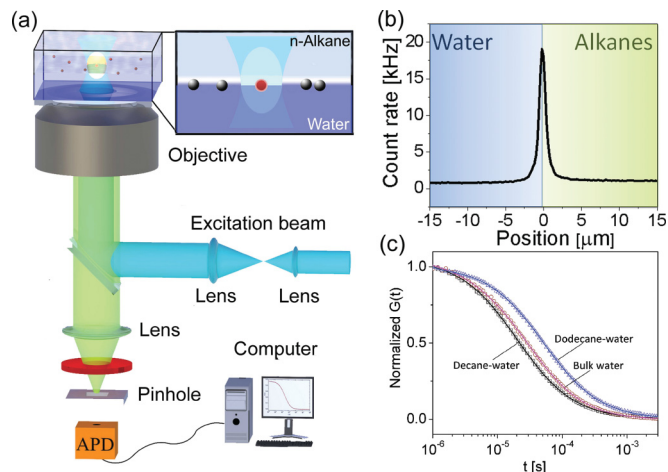


FIG. 2. (Color online) (a) Schematic of the FCS setup. (b) A fluorescence intensity scan through a water-*n*-decane interface on which rhodamine is adsorbed. Scanning was carried out by moving the focus from water into the *n*-alkane phase in steps of 200 nm. (c) Typical autocorrelation curves and their representation with Eq. (1) (solid lines) for rhodamine diffusing at water-decane (black squares) and water-dodecane (blue triangles) interfaces. The autocorrelation curve for rhodamine diffusing in bulk water (magenta circles) is shown for comparison.

saturation after ~ 5 min at a typical surface coverage of $0.5 \mu\text{m}^2$ per molecule.

FCS experiments were done using a commercial setup comprising the module ConfoCor2 and an inverted microscope Axiovert 200, (Carl Zeiss, Germany). The fluorescent molecules were excited by the 488-nm line of an argon laser focused in the middle of the interfaces [Fig. 2(a)] by a water immersion microscope objective, C-Apochromat $40\times$, NA 1.2 (Carl Zeiss, Germany). The fluorescent light was collected by the same objective, passed a confocal pinhole and LP530 long pass emission filter, and finally directed to an avalanche photodiode detector that enabled single-photon counting. This arrangement results in the formation of a confocal detection volume V_d around the laser focus. The detection volume has a three-dimensional (3D) Gaussian shape and typical dimension of ~ 300 nm in the radial direction and $1.5 \mu\text{m}$ in the normal direction [24]. Only the fluorescence originating from species within V_d can be delivered to and detected by the avalanche photodiode detector.

The confocal detection volume was scanned across the interface (in 200-nm steps) by moving the microscope objective that is mounted on a high-precision electromechanical stage. No fluorescence could be detected if V_d was moved away from the interface [Fig. 2(b)], which indicates that there were negligibly few fluorescent molecules diffusing in the bulk aqueous or *n*-alkane phases. As a next step, V_d was positioned exactly at the interface, i.e., at the point of maximum fluorescence intensity [Fig. 2(b)]. The fluctuations $\delta F(t) = F(t) - \langle F(t) \rangle$ of the fluorescence intensity $F(t)$ caused by the interfacial diffusion of the tracer molecules through the confocal detection volume were recorded and evaluated in terms of an autocorrelation function $G(t) = \langle \delta F(t') \delta F(t' + t) \rangle / \langle F(t') \rangle^2$ [Fig. 2(c)]. For each sample a series of 6–18 independent autocorrelation curves were measured (50 s

each) and averaged; data sets influenced by occasional large aggregates were excluded. The experiments were repeated at least five times on different days with freshly prepared samples.

For the case of two-dimensional diffusion considered here the autocorrelation function has the form [24]

$$G(t) = 1 + \left[1 + \frac{X_{Tr}}{1 - X_{Tr}} e^{-t/\tau_{Tr}} \right] \frac{1}{N} \frac{1}{\left[1 + \frac{t}{\tau_D} \right]}. \quad (1)$$

Here, N is the average number of diffusing molecules in the focal volume that is reversely proportional to the surface coverage, X_{Tr} and τ_{Tr} are the fraction and the decay time of the triplet state, and τ_D is the diffusion time. It is directly related to the two-dimensional diffusion coefficient by $D_{||} = x_0^2/4\tau_D$. Here $x_0 = 220$ nm is the lateral dimension of the confocal detection volume, V_d . It was determined by measuring the diffusion time of rhodamine in bulk water and using the literature value for its diffusion coefficient (3.82×10^{-10} m²/s at 22 °C [30]).

III. RESULTS

Typical autocorrelation curves measured for rhodamine, PDI1, and the dendrimer diffusing at various water- n -alkane interfaces are shown in Figs. 2(c) and 3. The values of the

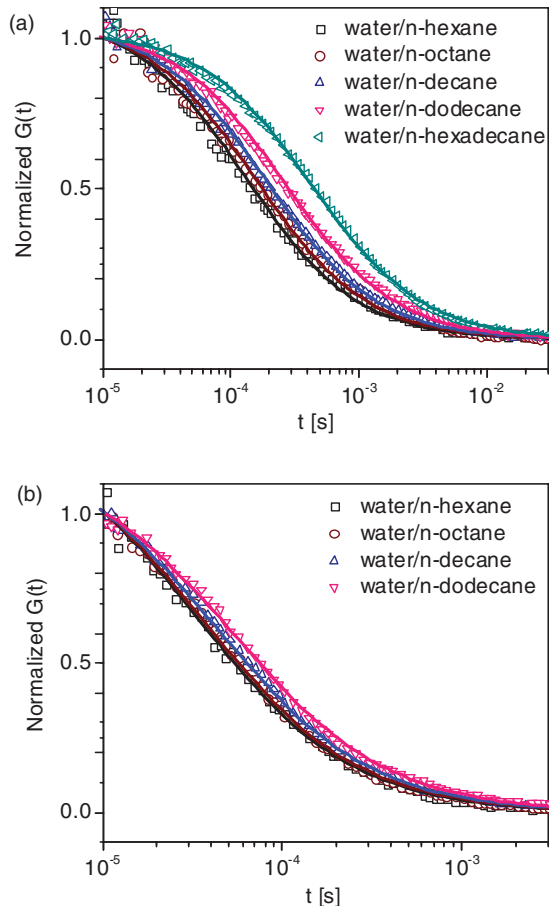


FIG. 3. (Color online) Normalized autocorrelation curves of (a) dendrimer and (b) PDI1 diffusing at various water-alkane interfaces and the corresponding fits with Eq. (1) in the main text (solid lines).

interfacial diffusion coefficients $D_{||}$ obtained for all tracers diffusing at the studied water- n -alkane interfaces are plotted versus the n -alkane viscosity in Fig. 4(a).

A. Large tracers

For the large dendrimer tracers ($R_H = 4.0$ nm) a gradual decrease of $D_{||}$ with alkane viscosity η_a was observed [circles in Fig. 4(a)]. In first approximation to a more complex theory [31] the diffusion coefficient of tracer molecules along the fluid-fluid interface is described by the Stokes-Einstein relation for spherical particles. Here we assumed that the viscous drag on the sphere can be approximated as the sum of contributions from the water and the alkane phases. The relative weighting of each contribution is given by the cross-sectional area of the sphere in the respective phase [Fig. 4(b)]. The position of the three-phase contact line is characterized by the contact angle Θ . The cross-sectional area of the sphere in the alkane phase is $A_a = R^2(2\Theta - \sin 2\Theta)/2$, and that in the water phase is $A_w = \pi R^2 - A_a$. With this simple model we can estimate the dependence of the diffusion coefficient on the viscosities

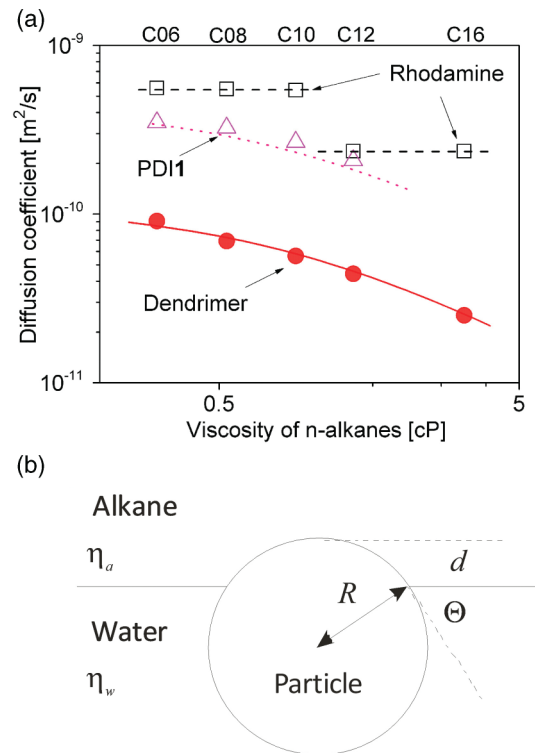


FIG. 4. (Color online) (a) Interfacial diffusion coefficient $D_{||}$ versus viscosity of the alkane phase measured for the dendrimer (solid circles), PDI1 (triangles) and rhodamine (squares) molecules at various water-alkane interfaces. The dashed line is a guide to the eye for rhodamine. The continuous line represents the values obtained with Eq. (2) for the dendrimer using $R = 4.0$ nm and $\Theta = 90^\circ$. The dotted line represents Eq. (2) with $R = 1.0$ nm and $\Theta = 90^\circ$ for the PDI1. The C_j on the top of the figure indicates the carbon number of the alkane used. The error bars evaluated from the statistical deviations of the measurements are smaller than the symbol size. (b) Schematic of a spherical particle at a water-alkane interface.

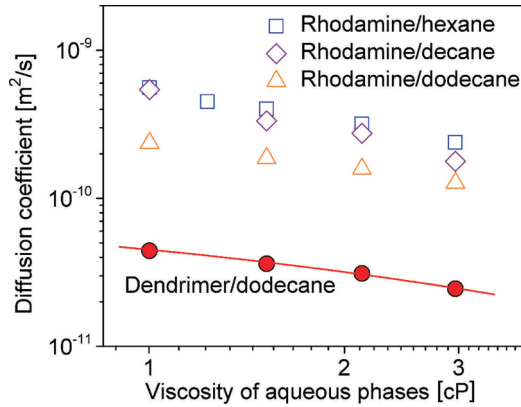


FIG. 5. (Color online) Interfacial diffusion coefficient versus viscosity of the aqueous phase for rhodamine tracers at aqueous-hexane (open squares), aqueous-decane (open diamonds), and aqueous-dodecane (open triangles) interfaces. The solid circles represent the dendrimer tracers diffusing at aqueous-dodecane interfaces. The viscosity of the aqueous phase was adjusted by mixing water with glycerol.

of the two phases:

$$D_A = \left(\frac{kT}{6\pi R} \right) \left[\frac{2\pi}{2\pi\eta_w + (\eta_a - \eta_w)(2\Theta - \sin 2\Theta)} \right]. \quad (2)$$

The diffusion of the dendrimers could be well represented [solid line in Fig. 4(a)] with Eq. (2) using a contact angle value of $\Theta = 90^\circ$ and a sphere radius $R = 4.0$ nm, a value that is equal to the experimentally measured hydrodynamic radius of the dendrimer. In the particular case of the water-decane interface, where the viscosities of the two phases— $\eta_w = 0.96$ cPa s for water and $\eta_a = 0.90$ cPa s for decane—are very similar, the value of D_{\parallel} was equal to the diffusion coefficient of 5.6×10^{-11} m²/s measured in bulk water.

To get further insight we also measured the lateral diffusion coefficient D_{\parallel} of the dendrimers versus the viscosity of the polar (aqueous) phase (solid circles in Fig. 5). The viscosity was adjusted by adding different amounts of glycerol. D_{\parallel} can be described by Eq. (2) using the same R of 4.0 nm and the same contact angle of 90° (the solid line in Fig. 5). This observation is readily explained by an almost equal immersion of the large dendrimer molecules in the aqueous and alkane phases.

B. Small molecular tracers

The lateral diffusion of the smaller PDII molecules ($R_H = 1.0$ nm) at various water-alkane interfaces was also studied. D_{\parallel} of PDII showed a gradual decrease with the increase of the alkane phase viscosity [Fig. 4(a)]. This indicates that the PDII molecules penetrate in both phases similar to what was observed for the dendrimer tracers. However, in contrast to the larger dendrimers ($R_H = 4.0$ nm), the experimentally measured values of D_{\parallel} for the PDII are systematically higher than the prediction of Eq. (2) for a contact angle of 90° [Fig. 4(a)]. Furthermore, these experimental data cannot be represented by Eq. (2) for any value of the contact angle. Finally and most importantly, at the water-decane interface, where the viscosities of both phases are almost equal, PDII

molecules diffuse approximately 1.15 times faster than in bulk water. This indicates that in contrast to the larger dendrimers, the small PDII tracers sense the presence of a very thin interfacial layer with reduced effective viscosity.

The existence of such layer is further confirmed by the diffusion data for the smallest ($R_H = 0.6$ nm) rhodamine tracers. At the water-decane interface, the rhodamine diffuses approximately 1.4 times faster than in bulk water. Moreover, as shown in Fig. 4(a), the rhodamine tracers exhibit a qualitatively different dependence of D_{\parallel} on the alkane phase. While its viscosity is changing gradually by one order of magnitude between hexane and hexadecane, the value of D_{\parallel} was constant (5.5×10^{-10} m²/s) for alkanes with up to ten carbon atoms. Between decane and dodecane the diffusion coefficient decreased to 2.4×10^{-10} m²/s. Then it remained constant up to hexadecane. Clearly this stepwise behavior cannot be represented by Eq. (2). In contrast, D_{\parallel} of rhodamine showed a continuous dependence on the viscosity of the aqueous phase (Fig. 5). However, this dependence also cannot be represented by Eq. (2).

C. Possible artifacts

Before further discussion, it is important to address some effects that may possibly cause artifacts and errors in the interpretation of the experimental results. First of all, we should consider the accuracy of FCS in measuring the interfacial diffusion coefficients of the tracers, D_{\parallel} . As discussed in Sec. II the diffusion coefficient is calculated through $D_{\parallel} = x_0^2/4\tau_D$, where τ_D is the diffusion time of the tracers and x_0 is the lateral dimension of the confocal detection volume. While τ_D can be reliably and reproducibly obtained by fitting the experimental autocorrelation curves with Eq. (1), the precise value of x_0 is not well known. It depends strongly on the geometrical characteristics of the optical setup and the refractive index (n_s) of the sample, and therefore an appropriate calibration is necessary. Typically this is done by measuring and fitting the autocorrelation curves for freely diffusing (3D diffusion in bulk samples) dye molecules with known diffusion coefficient, e.g., rhodamine in water. For the two-dimensional (2D) diffusion at water-alkane interfaces, however, the accuracy of this procedure is not self-evident. Indeed, while the calibration is done in pure water, during the 2D measurements the focus is partially positioned in the alkane phase, which has a higher refractive index than water. This may cause optical distortions and result in a small change in the lateral dimension of the detection volume and thus a systematic error in the estimated values of the interfacial diffusion coefficient. Furthermore, as the different alkanes have slightly different refractive indices, the eventual error may depend on the alkane length. In order to estimate the magnitude of these effects we have measured the diffusion time of organic quantum dots, 545 ITK (Invitrogen, Leiden, Netherlands), with a hydrodynamic radius of 4.7 nm in all alkanes, using the same water immersion objective as for the 2D studies. The plot of the diffusion time against the alkane viscosity is shown in Fig. 6. The dashed line in the figure represents the value of the diffusion time calculated on the basis of the Stokes-Einstein equation assuming the same lateral dimension of the observation volume for all alkanes. As can be seen there is a remarkable agreement between the

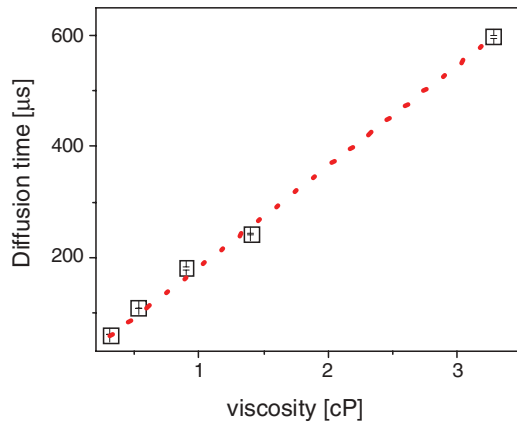


FIG. 6. (Color online) Diffusion time of quantum dots in bulk alkanes as a function of viscosity of alkanes; the red, dotted line represents the prediction of the Stokes-Einstein equation.

experimental data and the theoretical prediction [24,32]. Thus, the results presented in Fig. 6 show that changing the refractive index from 1.37 for hexane to 1.43 for hexadecane has only a minor effect (less than 5%) on the detection volume size. As the refractive index of water, 1.33 is only slightly smaller than that of hexane; we estimate that the error in the calibration of the lateral dimension of the detection volume is less than 5%. We conclude that even if optical distortions cause systematic error in the estimated values of the interfacial diffusion coefficient, this error is small and does not depend on the carbon number of alkanes.

Another possible effect that can influence the tracers' diffusion is the presence of surface active contamination in the studied solutions. This was ruled out by measuring the interfacial tension of all water-alkane interfaces. The obtained values (Table I) are in good agreement with those reported in the literature [33], confirming that there were no surface active compounds in the used solvents. Nevertheless in order to clarify the effect of such compounds on our results, in a

TABLE I. Interfacial tension of water-*n*-alkanes ($T = 20^\circ\text{C}$).

<i>n</i> -Alkane	γ (Water- <i>n</i> -alkane) (mN/m) ^a	γ (Water- <i>n</i> -alkane) (mN/m) ^{b,c}
<i>n</i> -Hexane	50.80	49.7 ± 0.1
<i>n</i> -Octane	51.64	50.6 ± 0.1
<i>n</i> -Decane	52.33	51.4 ± 0.1
<i>n</i> -Dodecane	52.87	51.7 ± 0.1
<i>n</i> -Hexadecane	–	52.4 ± 0.1

^aReference [26].

^bAll interfacial tension measurements reported in this work were done using a software controlled Du-Noüy ring tensiometer (ring height = 25 mm, ring diameter = 18.7 mm, and wire thickness = 0.37 mm; Data Physics Instruments, Germany). Samples were measured in a 50-cm³ measuring cell at a temperature 293 ± 0.5 K. Each value reported in the table is an average of ten measurements with an accuracy of ± 0.05 mN/m.

^cOur control experiments at water-octane, water-decane, and water-dodecane interfaces showed that one and the same value of interfacial tension was measured for purified liquids or after degassing within statistical error.

separate experiment we purposefully added sodium dodecylsulfate or cetyl trimethylammonium bromide with concentrations of 10^{-6} M into the aqueous phases, and measured the diffusion of rhodamine at a water-decane interface. We found that the presence of surfactants, independent of their surface charge, resulted in a significant decrease (and not an increase) of the interfacial diffusion coefficient. This finding confirms that our results are not affected by eventual contaminations.

As the rhodamine molecules carry a positive charge, the electrostatic interactions between the molecules may also affect their diffusion. Clearly increasing the rhodamine concentration at the interface should increase the effect of the electrostatic interactions. FCS experiments provide independent information on the tracer concentration at the interface. In a typical measurement, the area per molecule was approximately $0.5 \mu\text{m}^2$. Our control experiment showed that when the area per molecule was $0.003 \mu\text{m}^2$, the diffusion coefficient of rhodamine at a water-decane interface was approximately 15% less than the value measured when the area per molecule was $0.5 \mu\text{m}^2$. In addition, we tested the effect of salt by measuring the diffusion coefficient of rhodamine at a water-decane interface and adding 10 mM KCl into the aqueous phase. The diffusion coefficient did not change. This indicates that the electrostatic forces do not affect the measured interfacial diffusion coefficients.

IV. DISCUSSION

After testing and excluding the effect of various possible artifacts, we now turn to interpretation of the experimental data. Our results support the following model: At the water-alkane interface there is a reduced viscosity layer. Rhodamine at the interface is continuously located towards the aqueous phase while PDI1 and dendrimers span across the interface (Fig. 7). A different, but in both cases significant, fraction of the cross-section of each rhodamine and PDI1 molecule is located within this high-mobility and high-entropy region. As a result they experience different degrees of the reduced effective viscosity and diffuse faster than in bulk. A reason for the existence of this high-mobility region could be the presence of dangling OH bonds at the water-alkane interface [4,5]. This picture is supported by recent nonlinear spectroscopy studies that found ultrafast reorientational motion of water molecules at the air-water interface [34,35]. The larger dendrimer tracers with a hydrodynamic radius of 4.0 nm are symmetrically

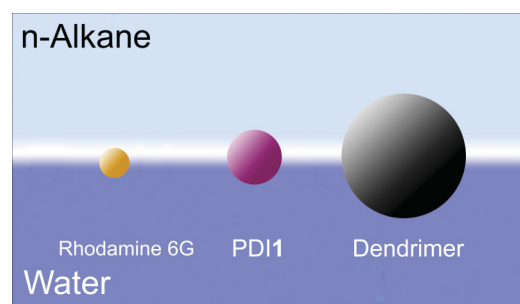


FIG. 7. (Color online) Schematic illustrating the positions of the studied tracers at the water-alkane interfaces. The white region represents the reduced viscosity layer.

immersed in both the aqueous and the alkane phases. Their size is much larger than the 2–4 Å correlation length in bulk water [36,37] that provides the natural length scale over which structural anomalies at interfaces tend to decay [38–40]. As a consequence, dendrimer diffusion is not significantly affected by the reduced viscosity layer and could be adequately represented by the bulk viscosity values of the surrounding liquid phases.

This model explains our experimental observations for PDI1 and dendrimer diffusion on all studied water-alkane interfaces and the rhodamine diffusion on the water-hexane, water-octane, and water-decane interfaces. However, for rhodamine diffusing at the longer alkanes-water interfaces, i.e., dodecane and hexadecane, the situation is more complex. As shown in Fig. 4(a), for these alkanes D_{\parallel} of rhodamine decreases stepwise to a value of 2.36×10^{-10} m²/s. This is even lower than the diffusion coefficient in bulk water (3.82×10^{-10} m²/s at 22 °C).

In the following we discuss the relevant length scales that appear at the water-oil interface, relating them to phenomena that can explain the stepwise slowdown of interfacial diffusion. The capillary wave theory predicts the interfacial width of water-alkane by [41]

$$\sigma^2 = \frac{1}{4} B \ln [(q_u^2 + \kappa^2)/\kappa^2]. \quad (3)$$

Here, σ^2 is the total intrinsic mean-square surface displacement; $B = k_B T / \pi \gamma$ where k_B is the Boltzmann constant, T is the temperature, γ is the surface tension at T ; the upper cutoff $q_u = 1 \text{ \AA}^{-1}$ is provided by the typical molecular length scale $2\pi/q_u$; the gravitational cutoff $\kappa^2 = \Delta\rho g / \gamma$, where $\Delta\rho$ is the difference in mass density across the interface and g is the gravitational acceleration. Then, the total intrinsic mean-square surface displacement σ of water-alkane is 6.8 Å. Thus for our water-alkane interfaces, the dynamic contribution from capillary wave theory to the interfacial width that could potentially affect interfacial diffusion is approximately 7 Å. However, this value is almost identical for all investigated systems and therefore cannot explain the observed stepwise slow-down.

In water, the relevant length scale that leads to a disruption of the hydrogen-bond network is provided by the crossover from volume to surface scaling in the solvation free energy for hydrophobic cavities. This value of approximately 10 Å is indicative for the curvature of an interface that allows elastic rearrangement of the water molecules, thus distorting rather than breaking their hydrogen-bonding network [1]. However, this transition happens gradually and therefore is unlikely to cause the sudden change observed by FCS. Moreover, opposite to what was observed experimentally, one would expect a slower diffusion near partially solvated short chain n -alkanes

that leave the water structure intact, versus faster diffusion at longer alkanes where the formation of an interfacial depletion layer becomes more likely due to the increased number of broken bonds near larger objects.

The next important scale in the problem is given by the size of the rhodamine molecule, i.e., $R_H = 0.6$ nm or its physical radius that is around 0.3–0.4 nm. For alkanes, the radius of gyration provides the characteristic length scale that governs interfacial properties such as the intrinsic width [22]. The diffusion slowdown happens between decane and dodecane that have radii of gyration of 3.0 and 3.5 Å, respectively. Considering these length scales indicates that the stepwise decrease of D_{\parallel} coincides with alkane coil size that matches the size of rhodamine. This finding is also consistent with earlier fluorescence recovery after photobleaching studies of Kovaleski and Wirth [42], which indicated that not the viscosity of alkanes, but rather the interfacial roughness is slowing down the lateral diffusion at water-alkane interfaces. Such assumption can explain our results, supposing that the decrease of the rhodamine diffusion coefficient (as compared to the bulk water value) on the water-dodecane and water-hexadecane interfaces is overcompensated from a slowdown resulting from, e.g., the interfacial roughness. Finally, it should be mentioned that in contrast to the rhodamine, the PDI1 molecules were not directly affected by the interfacial roughness and did not show a stepwise change in D_{\parallel} with alkane viscosity. This is related to the fact that the larger and more amphiphilic PDI1 molecules penetrate in both phases, i.e., they span across the interface and thus their diffusion is not directly influenced by the gyration radii of alkanes.

V. CONCLUSIONS

To conclude, we report a strategy to study the controversial question of the existence and the properties of interfacial water adjacent to a hydrophobic surface. Rather than measuring structural and spectroscopic properties we directly probe the interfacial dynamics via the diffusion coefficient of single-molecular tracers as a function of viscosity of both liquid phases and the tracer's size. Our results indicate the existence of an interfacial region with reduced effective viscosity and increased mobility that decays over a length scale on the order of a water monolayer towards bulk dynamics.

ACKNOWLEDGMENTS

The authors acknowledge financial support from DFG (Grant No. SPP1259 KO3747/3-1). C.Y.L. is grateful to the support of the Alexander von Humboldt Foundation.

-
- [1] D. Chandler, *Nature* **437**, 640 (2005).
 [2] S. Granick and S. C. Bae, *Science* **322**, 1477 (2008).
 [3] S. Sastry, *Nature* **409**, 300 (2001).
 [4] Q. Du, E. Freysz, and Y. R. Shen, *Science* **264**, 826 (1994).
 [5] L. F. Scatena, M. G. Brown, and G. L. Richmond, *Science* **292**, 908 (2001).
 [6] M. Sovago, R. K. Campen, G. W. H. Wurpel, M. Müller, H. J. Bakker, and M. Bonn, *Phys. Rev. Lett.* **100**, 173901 (2008).
 [7] I. V. Stiopkin, C. Weeraman, P. A. Pieniazek, F. Y. Shalhout, J. L. Skinner, and A. V. Benderskii, *Nature* **474**, 192 (2011).
 [8] F. H. Stillinger, *J. Solution Chem.* **2**, 141 (1973).

- [9] K. Lum, D. Chandler, and J. D. Weeks, *J. Phys. Chem. B* **103**, 4570 (1999).
- [10] T. R. Jensen, M. O. Jensen, N. Reitzel, K. Balashev, G. H. Peters, K. Kjaer, and T. Bjornholm, *Phys. Rev. Lett.* **90**, 086101 (2003).
- [11] M. Mezger, H. Reichert, S. Schoder, J. Okasinski, H. Schroder, H. Dosch, D. Palms, J. Ralston, and V. Honkimaki, *Proc. Natl. Acad. Sci. USA* **103**, 18401 (2006).
- [12] A. Poynor, L. Hong, I. K. Robinson, S. Granick, Z. Zhang, and P. A. Fenter, *Phys. Rev. Lett.* **97**, 266101 (2006).
- [13] M. Mezger, F. Sedlmeier, D. Horinek, H. Reichert, D. Pontoni, and H. Dosch, *J. Am. Chem. Soc.* **132**, 6735 (2010).
- [14] M. Maccarini, R. Steitz, M. Himmelhaus, J. Fick, S. Tatur, M. Wolff, M. Grunze, J. Janecek, and R. R. Netz, *Langmuir* **23**, 598 (2007).
- [15] C. Sendner, D. Horinek, L. Bocquet, and R. R. Netz, *Langmuir* **25**, 10768 (2009).
- [16] B. M. Ocko, A. Dhinojwala, and J. Daillant, *Phys. Rev. Lett.* **101**, 039601 (2008).
- [17] M. Mezger, S. Schöder, H. Reichert, H. Schröder, J. Okasinski, V. Honkimäki, J. Ralston, J. Bilgram, R. Roth, and H. Dosch, *J. Chem. Phys.* **128**, 244705 (2008).
- [18] R. Vácha, D. Horinek, M. L. Berkowitz, and P. Jungwirth, *Phys. Chem. Chem. Phys.* **10**, 4975 (2008).
- [19] C. D. Wick, T. M. Chang, J. Slocum, and O. T. Cummings, *J. Phys. Chem. C* **116**, 783 (2012).
- [20] H. S. Ashbaugh, L. R. Pratt, M. E. Paulaitis, J. Clohacy, and T. L. Beck, *J. Am. Chem. Soc.* **127**, 2808 (2005).
- [21] F. Bresme, E. Chacón, P. Tarazona, and K. Tay, *Phys. Rev. Lett.* **101**, 056102 (2008).
- [22] D. M. Mitrinovic, A. M. Tikhonov, M. Li, Z. Q. Huang, and M. L. Schlossman, *Phys. Rev. Lett.* **85**, 582 (2000).
- [23] K. Kashimoto, J. Yoon, B. Y. Hou, C. H. Chen, B. H. Lin, M. Aratono, T. Takiue, and M. L. Schlossman, *Phys. Rev. Lett.* **101**, 076102 (2008).
- [24] R. Rigler and E. Elson, *Fluorescence Correlation Spectroscopy: Theory and Applications* (Springer Verlag, Berlin, 2001).
- [25] D. Wang, S. Yordanov, H. M. Paroor, A. Mukhopadhyay, C. Y. Li, H.-J. Butt, and K. Koynov, *Small* **7**, 3502 (2011).
- [26] A. Goebel and K. Lunkenheimer, *Langmuir* **13**, 369 (1997).
- [27] D. A. Doshi, E. B. Watkins, J. N. Israelachvili, and J. Majewski, *Proc. Natl. Acad. Sci. USA* **102**, 9458 (2005).
- [28] C. Kohl, T. Weil, J. Qu, and K. Müllen, *Chem. Eur. J.* **10**, 5297 (2004).
- [29] M. Yin, J. Shen, G. O. Pflugfelder, and K. Muellen, *J. Am. Chem. Soc.* **130**, 7806 (2008).
- [30] C. Müller, A. Loman, V. Pacheco, F. Koberling, D. Willbold, W. Richtering, and J. Enderlein, *Europhys. Lett.* **83**, 46001 (2008).
- [31] T. M. Fischer, P. Dhar, and P. Heinig, *J. Fluid Mech.* **558**, 451 (2006).
- [32] M. Eigen and R. Rigler, *Proc. Natl. Acad. Sci. USA* **91**, 5740 (1994).
- [33] S. Zeppieri, J. Rodriguez, and A. L. L. de Ramos, *J. Chem. Eng. Data* **46**, 1086 (2001).
- [34] J. A. McGuire and Y. R. Shen, *Science* **313**, 1945 (2006).
- [35] C. S. Hsieh, R. K. Campen, A. C. Vila Verde, P. Bolhuis, H. K. Nienhuys, and M. Bonn, *Phys. Rev. Lett.* **107**, 116102 (2011).
- [36] L. Bosio, J. Teixeira, and H. E. Stanley, *Phys. Rev. Lett.* **46**, 597 (1981).
- [37] Y. Xie, K. F. Ludwig, Jr., G. Morales, D. E. Hare, and C. M. Sorensen, *Phys. Rev. Lett.* **71**, 2050 (1993).
- [38] O. Magnussen, B. Ocko, M. Regan, K. Penanen, P. Pershan, and M. Deutsch, *Phys. Rev. Lett.* **74**, 4444 (1995).
- [39] D. S. Walker and G. L. Richmond, *J. Am. Chem. Soc.* **129**, 9446 (2007).
- [40] M. Mezger, H. Schröder, H. Reichert, S. Schramm, J. S. Okasinski, S. Schöder, V. Honkimäki, M. Deutsch, B. M. Ocko, J. Ralston, M. Rohwerder, M. Stratmann, and H. Dosch, *Science* **322**, 424 (2008).
- [41] M. K. Sanyal, S. K. Sinha, K. G. Huang, and B. M. Ocko, *Phys. Rev. Lett.* **66**, 628 (1991).
- [42] J. M. Kovalski and M. J. Wirth, *J. Phys. Chem.* **99**, 4091 (1995).